Available online at www.sciencedirect.com

ScienceDirect

Nuclear Physics A 930 (2014) 131–138

NUCLEAR PHYSICS A

www.elsevier.com/locate/nuclphysa

Is there incomplete fusion mechanism beyond 100*A* MeV?

P. Eudes [a], Z. Basrak [b,*], V. de la Mota [a], G. Royer [a]

[a] *SUBATECH, EMN-IN2P3/CNRS-Université de Nantes, Nantes, France*
[b] *Ruđer Bošković Institute, Zagreb, Croatia*

Received 4 June 2014; received in revised form 21 July 2014; accepted 22 July 2014

Available online 28 July 2014

Abstract

Presented is a universal description of the generalized fusion excitation function which indicates that the fusion reaction mechanism should vanish at center-of-mass energy per nucleon of about 13 MeV/nucleon independently of the specific heavy-ion reaction system. Placing reliance on this result and comforted by semiclassical transport model simulations we suggest that the proposed persistence of the incomplete fusion cross sections in the measurement of the ^{14}N induced reactions on heavy targets at beam energies between 100*A* and 155*A* MeV should be attributed to a geometrical participant-spectator-like reaction mechanism.

Keywords: Heavy-ion reactions; Intermediate energies; Fusion excitation function; Vanishing of fusion; Semiclassical transport model; Geometrical participant-spectator picture

1. Introduction

Fusion reaction mechanism is related to the formation of a fully equilibrated nuclear system which may be either the result of amalgamating all the nucleons into a compound nucleus (complete fusion, CF) or of only a part of the total reaction system (incomplete fusion, IF). According to the strong absorption picture of nuclear processes the fusion, or more generally

* Corresponding author.
E-mail address: basrak@irb.hr (Z. Basrak).

http://dx.doi.org/10.1016/j.nuclphysa.2014.07.035
0375-9474/

the total reaction cross section, may be approximated by a simple schematic relation between center-of-mass energy $E_{\mathrm{c.m.}}$, reaction threshold barrier V and an effective interaction radius R:

$$\sigma(E) = \pi R^2 \left(1 - \frac{V}{E_{\mathrm{c.m.}}}\right). \tag{1}$$

Each empirical model, from the first one by Bass [1], intended to describe the fusion cross section σ_{fus} relies on the above functional form. According to Eq. (1), σ_{fus} expressed as a function of $1/E_{\mathrm{c.m.}}$ increases linearly with increasing energy. Such a behavior characterizes the so-called fusion region I.

At E_{inc} several times higher than the barrier the fusion starts to compete not only with transfer, inelastic and quasi-elastic processes but progressively with strongly damped processes which do not lead to compound-nucleus formation. Fusion is still the dominant reaction mechanism but σ_{fus} stagnates. This region is referred to as the fusion region II. With the further rise of energy sequential and simultaneous fragmentation processes open. In addition, the reaction system is exposed to conditions at which energetic particles may leave the composite system at the early collision stage and, thus, reduce the mass of the eventually formed compound nucleus. One is dealing with the fusion region III in which both CF and IF are present. Although the IF mechanism after opening increases, in the region III the total σ_{fus} steadily decreases with the rise of E_{inc}, quickly ceases to be a dominant reaction mechanism and ends by vanishing. A recent review on heavy-ion reaction mechanisms may be found in Ref. [2] and specifically on the fusion reactions in Ref. [3].

In a recent publication [4] we have demonstrated that the fusion region III cross sections reduced by the reaction cross section $\sigma_{\mathrm{red}} = \sigma_{\mathrm{fus}}/\sigma_{\mathrm{reac}}$ as a function of the center-of-mass energy per nucleon, i.e. the so-called (system) available energy

$$E_{\mathrm{avail}} = \frac{E_{\mathrm{c.m.}}}{A_{\mathrm{sys}}} = \frac{E_{\mathrm{lab}}}{A_{\mathrm{p}}} \frac{A_{\mathrm{p}} A_{\mathrm{t}}}{(A_{\mathrm{p}} + A_{\mathrm{t}})^2}, \tag{2}$$

follows a universal homographic functional dependence

$$\sigma_{\mathrm{red}} = a + \frac{b}{E_{\mathrm{avail}} + c}. \tag{3}$$

This relation is derived by a direct application of the strong absorption model (1) to both σ_{fus} and σ_{reac} [4] while its universality is an outcome of the above energy scaling given by Eq. (2). In Eq. (2) A_p and A_t stand for projectile and target mass numbers, respectively, whereas incident energy reads $E_{\mathrm{inc}} = E_{\mathrm{lab}}/A_p$.

A fit with the homographic probe-function (3) presented in Ref. [4] has been carried out over the evaporation-residue σ_{fus} data only. A fit result over the full evaporation-residue and fusion–fission data set will be presented in Ref. [5] together with a fit over the portion of the full data set associated with the fusion region III. The latter consists of the 256 σ_{fus} data values belonging to 78 reaction systems whose fit coefficients are displayed in Table 1. The data span the mass asymmetry parameter $\mu = |A_t - A_p|/(A_t + A_p)$ between 0.0 and 0.886. The above fit function, within experimental errors, provides a common description of the fusion excitation function for an overwhelming amount of σ_{red} values and reaction systems [4,5]. In particular, from the relation (3) and Table 1 it follows that the fusion process completely disappears at $E_{\mathrm{avail}} = 13 \pm 1$ MeV/nucleon whatever the system characteristics are, regarding its mass, mass asymmetry or isospin content [4,5]. The two homographic functions [4] and [5] differ markedly less than their rather small uncertainties (cf. Table 1 and the orange background band around the

Table 1
Values of the best fit coefficients a, b and c of the homographic function (3) for the full fusion-data set of the fusion region III (taken from Table 4 of Ref. [5]). Reported are the uncertainties on the fit coefficients Δa, Δb and Δc too.

$a \pm \Delta a$	$b \pm \Delta b$	$c \pm \Delta c$
-0.0842 ± 0.0039	1.160 ± 0.049	0.516 ± 0.067

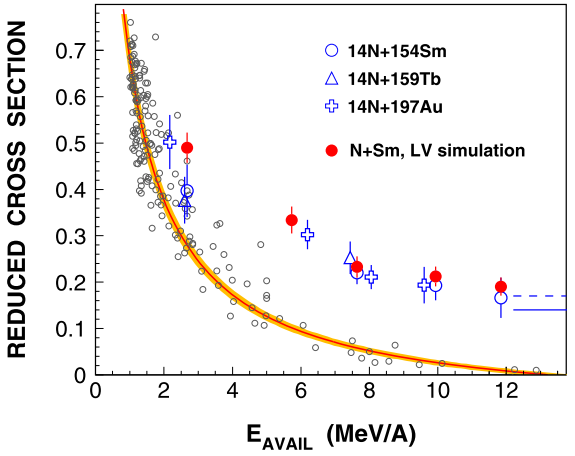

Fig. 1. (Color online.) Reduced fusion cross sections $\sigma_{\rm red}$ as a function of $E_{\rm avail}$. Open blue symbols refer to the experimental data of Ref. [6] and filled red circles to the LV simulation of the N + Sm reaction. The full red curve shows the universal homographic law of the scaled fusion excitation function, Eq. (3) with the parameter values listed in Table 1. The experimental data used in attaining this best fit curve are visualized by thin dark gray circles. For the figure clarity the experimental error bars are not drawn. The orange background band around the best fit curve is due to the errors on the fit parameters [5]. Horizontal thin full and dashed blue lines are due to Eq. (5) for the N + Sm and N + Au reactions, respectively.

best fit curve in Fig. 1) and both predicts strictly the same $E_{\rm avail}$ of the fusion disappearance. The goal of the present paper is to discuss those experimental results which are at odds with this universal feature of the fusion excitation function.

2. ^{14}N-induced reactions beyond 100A MeV

From the available literature we collected almost 400 fusion cross section data points at energies well above the barrier for fusion [4,5]. In Ref. [4] we discuss a bundle of 16 data points which are irregularly scattered within the $\sigma_{\rm red}$ vs. $E_{\rm avail}$ plane. These $\sigma_{\rm red}$ are lying considerably above the best-fit curve (3) and have $E_{\rm avail} < 5$ MeV/nucleon. Here we consider the only group of fusion data published so far which is systematically in conflict with the universal fusion excitation function (3): Sonzogni et al. [6] have investigated the ^{14}N-induced reactions at 35A, 100A, 130A and 155A MeV on the heavy targets ^{154}Sm, ^{159}Tb and ^{197}Au and have reported a nicely regular production cross sections (cf. in Fig. 1). Despite the high $E_{\rm inc}$ and rather large cross-section values the authors have attributed their observation to the incomplete fusion reaction mechanism. For instance, in the reaction ^{14}N(155A MeV) + ^{154}Sm they have found $\sigma_{\rm fus} = 460 \pm 120$ mb

(cf. Table I and Fig. 5 of Ref. [6]). This gives $\sigma_{\rm red} = 0.166 \pm 0.043$.[1] This value is more than 10 times above the expected one at $E_{\rm avail} = 11.84$ MeV/nucleon as may be inferred from Eq. (3), Table 1 and Fig. 1. Such a persistence of the fusion reaction mechanism, on one hand, and the nice regularity of the scaled cross sections $\sigma_{\rm red}$, on the other hand, suggests an extrapolation of the observed data trend beyond the measured energies. Making an asymptotical extrapolation one is led to conclude that fusion process would never extinct (cf. in Fig. 1). Such a result is in conflict with other available fusion data for both mass symmetric and mass asymmetric systems. For instance, the N + Tb point (open triangle in Fig. 1) at $E_{\rm avail} = 7.44$ MeV/nucleon with $\sigma_{\rm red} = 0.253 \pm 0.035$ is more than twice larger than the O + Au point of Ref. [8] which has been measured at $E_{\rm avail} = 7.43$ MeV/nucleon with $\sigma_{\rm red} = 0.110 \pm 0.012$, a value which lies on the homographic best-fit function [5].

To the best of our knowledge, the persistence of an incomplete fusion-like process at beam energies higher than $100A$ MeV has not, on one side, been corroborated by other works and, on the other side, such a result is difficult to reconcile with a natural extinction of the fusion process at high energies owing to a doubtful validity of the concept of compound-nucleus formation at these high energies. With the increase of energy one expects that mean-field effects in heavy-ion reactions become increasingly dominated by nucleon–nucleon collisions and, consequently, by the reaction geometry. At these energies one expects the validity of other nuclear reaction concepts like the participant-spectator picture [9] of heavy-ion reactions and which has been propounded to describe the experimental observations above $\approx 100A$ MeV. Moreover, our theoretical results performed in the framework of the semiclassical Landau–Vlasov transport model [10] have indicated that the reaction geometry starts to play a decisive role much below that energy [11,12].

3. Reaction probability and entrance channel geometry

Let us apply a geometrical approach to the present reaction case. In a geometrical picture, a fusion-like reaction can occur for collisions with an impact parameter smaller than $b_{\rm max}$ which is the value still allowing a complete overlap between the projectile and the target. Within this approximation, the fusion cross section reads

$$\sigma_{\rm fus} = \pi b_{\rm max}^2 = \pi (R_t - R_p)^2 = \pi r_0^2 \left(A_t^{1/3} - A_p^{1/3}\right)^2, \tag{4}$$

where R_p (R_t) is projectile (target) radius. Assuming the strong-absorption geometrical formula for the reaction cross section $\sigma_{\rm reac} = \pi r_0^2 (A_t^{1/3} + A_p^{1/3})^2$, one gets

$$\left(\frac{\sigma_{\rm fus}}{\sigma_{\rm reac}}\right)_g = \left[1 - \frac{2}{1 + (\frac{A_t}{A_p})^{1/3}}\right]^2 = \left[1 - \frac{2}{1 + (\frac{1+\mu}{1-\mu})^{1/3}}\right]^2, \tag{5}$$

where the subscript g reminds the schematic geometrical character of this expression. Eq. (5) indicates that at high energies the reduced $\sigma_{\rm red}$ tends towards a value which only depends on the mass asymmetry μ. Note that for a more and more symmetric system this limit tends to zero. For the ^{14}N + ^{154}Sm and ^{14}N + ^{197}Au reactions Eq. (5) gives 0.14 and 0.17, respectively in very good agreement with the experimental values [6] extrapolated asymptotically (see the full and dashed horizontal blue lines in Fig. 1).

[1] Throughout this paper $\sigma_{\rm fus}$ is normalized by $\sigma_{\rm reac}$ calculated with the phenomenological formula due to Tripathi et al. [7], i.e. the same one which has been used to obtain the numerical values stated in Table 1 of the parameters of Eq. (3).

4. Dynamical simulation

Because this very crude geometrical picture predicts only the asymptotical $\sigma_{\rm red}$ value, a much more realistic semiclassical simulation was undertaken with the Landau–Vlasov (LV) dynamical model [10]. Semiclassical microscopic transport approaches of the Boltzmann's type have been successfully confronted with a considerable number of experimental observations [13]. The LV model self-consistently treats both the nuclear and the Coulomb mean-field potentials of the colliding system. The nuclear component is calculated with the D1–G1 momentum-dependent interaction due to Gogny ($K_\infty = 228$ MeV and the effective mass $m^*/m = 0.67$) [14]. Residual nucleon–nucleon (NN) interaction is treated in the Uehling–Uhlenbeck approximation taking the empirical isospin- and energy-dependent free-scattering NN cross-section values [15].

We investigate theoretically the N + Sm reaction given that it is the most refereed experimental system in Ref. [6]. At each incident energy a simulation was performed in a wide range of impact parameters b and with a very small step around the critical b-values for the processes studied. The probability for forming a single fragment in the exit channel as a function of b was calculated and translated in terms of the cross section. Their corresponding reduced values are shown in Fig. 1 with filled red circles.

4.1. Reaction mechanism

In the following we examine the LV simulation results of the N + Sm reaction at the two extreme energies. Fig. 2 displays equidistant density-profile contours in the center-of-mass reference frame projected onto the reaction plane for several times of the early reaction stage. To render apparent the transfer of matter from the projectile to the target the projectile density contours are colored. At 35A MeV we chose $b = 6.0$ fm, i.e. slightly larger than the $b_{\rm max}$ of Eq. (4) (see panels in the left column (a) in Fig. 2) and at 155A MeV $b_{\rm max} \approx b = 5.0$ fm (panels of column (b) in Fig. 2). We underline the fact that for more central collisions one does not remark fundamental differences in the global reaction features relative to those which we are going to discuss below. At 35A MeV even in the case shown in Fig. 2 corresponding to a genuine semiperipheral collision the projectile matter is quickly dissolved and absorbed by the target. One remarks a strong angular momentum transferred to the system as a whole causing a burst of pre-equilibrium particles which are ejected at very negative angles (see in column (a) the panel at $t = 90$ fm/c). Already at 170 fm/c (see the last panel of column (a)) the absorbed projectile matter (equivalent to about 8 nucleons) is homogeneously distributed within the target-like sub-system. The chemical equilibration takes much longer time to be established relative to the time needed to establish equilibrium in momentum space (cf. e.g. in Fig. 3 of Ref. [16]). We can conclude that even for this semiperipheral collision, at 35A MeV a compound nucleus is formed and, consequently, one is dealing with the incomplete fusion reaction mechanism.

At 155A MeV one faces a radically different reaction course: The projectile keeps both its entity and direction of motion by traveling through the target. There is no significant transfer of angular momentum. The collision is so violent that the projectile completely disintegrates and sweeps away a considerable amount of the target nucleons. A cloud of about 30 nucleons leaves the system and only about 3 nucleons are transferred from the projectile to the target. At this high energy nothing justifies the fusion scenario of Ref. [6]. On the contrary, at energies above 100A MeV the entrance channel geometry governs the probability to have a single-fragment in the reaction exit channel. The absolute values of cross-sections obtained in the LV simulation

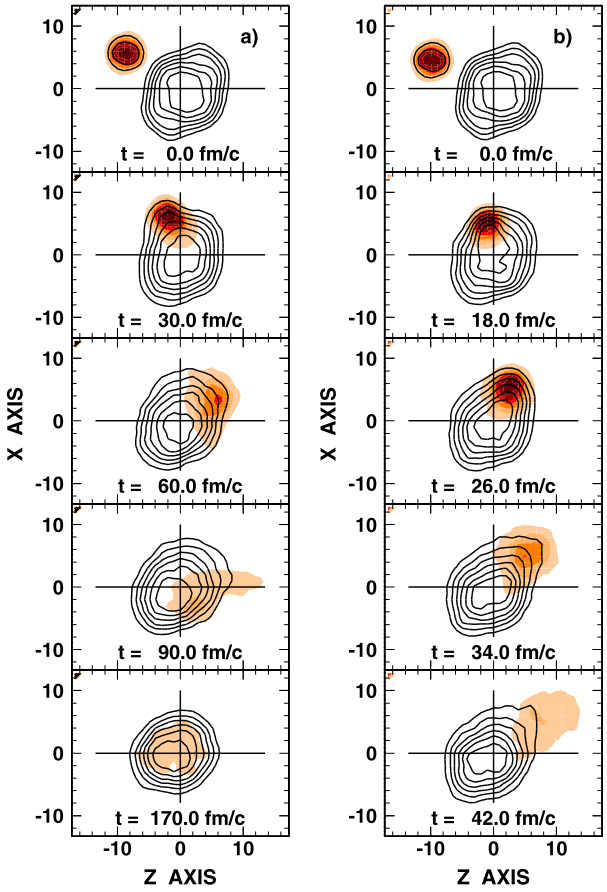

Fig. 2. (Color online.) Equidistant density-profile contours in the center-of-mass reference frame projected onto the reaction plane for the N + Sm LV simulation (a) at $E_{\text{inc}} = 35A$ MeV and $b = 6.0$ fm and (b) $E_{\text{inc}} = 155A$ MeV and $b = 5.0$ at selected times of the early reaction stage. In order to ease the pursue of the reaction evolution course the projectile density contours are colored. The z-axis is along the projectile direction.

are in full agreement with those obtained experimentally (see open blue and filled red circles in Fig. 1).

4.2. Linear momentum transfer

To refine our comparison between measured values and simulation results we also extracted the percentage of linear momentum transferred (LMT) to the composite system (see filled red circles connected by broken line in Fig. 3). This quantity is expressed as the ratio of the composite system velocity v, averaged over b, and the projectile velocity v_0, i.e. the same quantity as extracted experimentally and presented in Table II and Fig. 4 of Ref. [6]. They are displayed by open symbols referring to three ways of extracting the velocity ratio from the ^{14}N + ^{154}Sm data [6]. The Landau–Vlasov simulation satisfactorily compares with the experimental findings which is also an indirect proof that the LMT observation has been misinterpreted as resulting from an incomplete fusion process.

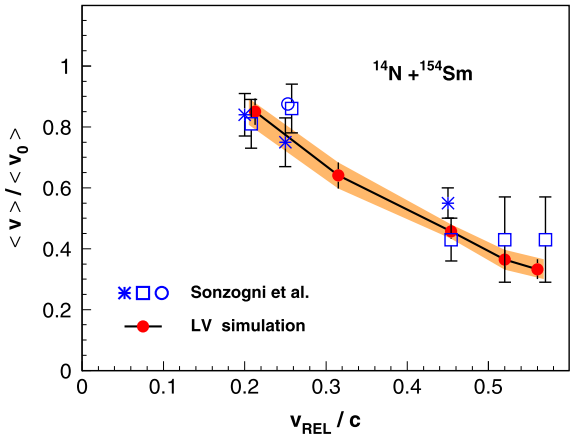

Fig. 3. (Color online.) Ratio of composite system velocity to entrance channel velocity as a function of the relative velocity at contact defined by $v_{\mathrm{REL}} = \sqrt{E_{\mathrm{inc}} - V_{\mathrm{Coul}}/A_p}$ for the N + Sm reaction. Open blue symbols refer to the experimental data of Ref. [6] and filled red circles to the LV simulation. Simulation points are connected with broken line to guide the eye while background orange zone depicts uncertainty.

5. Conclusion

In summary, the performed semiclassical transport simulations clearly demonstrate a crucial disparity between heavy-ion reaction mechanisms at incident energies 35A MeV and above 100A MeV for the highly mass asymmetric N + Sm system. The simulation correctly reproduces experimental cross sections and linear momentum transfer [6]. A simple estimation, just accounting for the entrance channel geometry, correctly reproduces the tendency of the data. Taking the above facts into account, we deduce that what have been measured in [6] may not be attributed to a fusion process. Fragment(s) observed in their experiment at $E_{\mathrm{inc}} \geq 100A$ MeV are due to a reaction mechanism which leads towards a pure geometrical participant-spectator-like reaction mechanism in which two-body degrees of freedom dominate over one-body ones. In these reactions above 100A MeV the most likely a moderately warm target-spectator-like fragment was formed rather than a fully equilibrated compound nucleus. The experiment left uncovered a huge gap in E_{inc}. It matters to remeasure such mass-asymmetric systems between 35A MeV and 100A MeV to pin down the evolution of heavy-ion reaction mechanism from fusion to the one dominated by reaction geometry. A corollary of such measurements could be a decisive contribution in revealing the underlying physical cause of fusion disappearance for very mass asymmetric systems. In particular, it will be interesting to learn whether the insufficient nuclear stopping, i.e. a kind of nuclear transparency, is responsible for fusion vanishing. Namely, in our study of the universal description of the fusion excitation function [4] the simulation results on moderately heavy systems having a relatively small asymmetry in mass (Ar + Ar, Ar + Ni and Ni + Ni) strongly indicate that nuclear transparency should be the cause of fusion vanishing, a phenomenon whose importance for the heavy-ion reaction mechanisms around and above the Fermi energy we have been advocating for some time [11,16,17]. Therefore, an experimental endorsement or disapproval of the advanced model explication for fusion disappearance is urgently needed as well as a verification whether this explanation of the extinction of fusion may be extended to fusion systems endowed by other mass characteristics.

Acknowledgements

Z.B. gratefully acknowledges the financial support and the hospitality of the Faculté des sciences of University of Nantes and the Laboratory SUBATECH.

References

[1] R. Bass, Nucl. Phys. A 231 (1974) 45.
[2] R. Planeta, Int. J. Mod. Phys. E 15 (2006) 973.
[3] B.B. Back, H. Esbensen, C.L. Jiang, K.E. Rehm, Rev. Mod. Phys. 86 (2014) 317.
[4] P. Eudes, Z. Basrak, F. Sébille, V. de la Mota, G. Royer, Europhys. Lett. 104 (2013) 22001.
[5] P. Eudes, Z. Basrak, F. Sébille, V. de la Mota, G. Royer, Phys. Rev. C, submitted for publication.
[6] A.A. Sonzogni, et al., Phys. Rev. C 53 (1996) 243.
[7] R.K. Tripathi, F.A. Cucinotta, J.W. Wilson, NASA Technical Paper 3621, 1997.
[8] H.A. Khan, T. Lund, P. Vater, R. Brandt, J.W.N. Tuyn, Phys. Rev. C 28 (1983) 1630.
[9] G.D. Westfall, et al., Phys. Rev. Lett. 37 (1976) 1202.
[10] C. Grégoire, et al., Nucl. Phys. A 465 (1987) 317;
F. Sébille, et al., Nucl. Phys. A 501 (1989) 137.
[11] P. Eudes, Z. Basrak, F. Sébille, Phys. Rev. C 56 (1997) 2003.
[12] I. Novosel, et al., Phys. Lett. B 625 (2005) 26.
[13] A. Bonasera, F. Gulminelli, J. Molitoris, Phys. Rep. 243 (1994) 1.
[14] J. Dechargé, D. Gogny, Phys. Rev. C 21 (1980) 1568.
[15] K. Chen, et al., Phys. Rev. 166 (1968) 949.
[16] Z. Basrak, Ph. Eudes, in: I. Iori (Ed.), Proceedings of the XXXVI Int. Winter Meeting on Nucl. Phys, Bormio, Italy, 1999, University of Milan Press, Milan, 1999, p. 284.
[17] Z. Basrak, P. Eudes, in: M. Korolija, Z. Basrak, R. Čaplar (Eds.), Proceedings of the International Conference on Clustering Aspects of Nuclear Structure and Dynamics, Rab, Croatia, 1999, World Scientific, 2000, p. 316.